IEEE Access
Multidisciplinary | Rapid Review | Open Access Journal

Received August 21, 2019, accepted September 1, 2019, date of publication September 4, 2019,
date of current version September 19, 2019.

Digital Object Identifier 10.1109/ACCESS.2019.2939511

Low-Profile Conformal UWB Antenna for UAV Applications

LUZ I. BALDERAS[1], ALBERTO REYNA[1,2], MARCO A. PANDURO[3], CARLOS DEL RIO[4], AND ARNULFO R. GUTIÉRREZ[1]

[1]Electrical and Electronic Engineering Department, University Autonomous of Tamaulipas, Reynosa 88779, Mexico
[2]Radanter SA DE CV, Reynosa 88620, Mexico
[3]CICESE Research Center, Ensenada 22860, Mexico
[4]Institute of Smart Cities, Public University of Navarre, 31006 Pamplona, Spain

Corresponding author: Alberto Reyna (alberto.reyna@uat.edu.mx)

This paper was supported by the Mexican Council for Science and Technology (CONACyT), under Grant no. 2016-01-1680.

ABSTRACT This article presents a new design of an ultra-wideband conformal antenna for Unmanned Aerial Vehicle (UAV) applications. The antenna is a low-profile structure which is very suitable to diminish aerial vehicle drag problem. The design utilizes Rogers Duroid 5880LZ material with dimensions of 29 mm $\times$ 39 mm. The measurement results show an ultrawideband performance of the $S_{11} < -10$dB from 2.9 GHz to 15.9 GHz. A Y-rounded shape achieves this frequency range with a parasitic circular element at the center of the structure. The acceptable radiation pattern performance is until 10.1 GHz, and the system fidelity factor is SFF > 0.9 in the maximum radiation. The proposed antenna was simulated and measured to test its performance when it is mounted on an UAV model.

INDEX TERMS Unmanned aerial vehicle, conformal antenna, UWB antenna.

I. INTRODUCTION

In recent years, Unmanned Aerial Vehicles (UAVs) have been used for exploration of the earth in emergency and surveillance catastrophic situations, for which it is necessary a signal detection system [1]. This application usually requires hardware to send high data transmission in ultrawideband (UWB) spectrum. The communications with UAVs are a big challenge because the instability and the drag issues when the drone is moving [2]. Furthermore, the UAV antenna system should be ultrawideband, low profile, and aerodynamic. In addition, it should have a directive pattern to the earth and spatial diversity. Typically, the UAV antennas are flat square patches and dipoles, which cannot be used for UWB applications [3]–[6]. Otherwise, the implementation of UWB technology on UAVs is feasible, as reported previously in [7]–[10]. Hence, the design problem of this research consists in finding out a UWB antenna design that can be located easily on the UAV with spatial diversity for the above UAV application. The antenna structure should be conformal to avoid drag problems that the UAV suffers during the flights.

Reviewing the literature of UWB conformal antennas, we can find some antenna designs manufactured with flexible materials on curve surfaces. For instance, a Vivaldi conformal antenna mounted on a pipe was proposed in [11]. This design works from 5.1 GHz to 11 GHz. A conformal volcano antenna was designed in [12]. This antenna shows an ultrawideband performance from 4.2 GHz to 8 GHz. A conformal exponential tapered slot antenna was proposed by using a liquid crystal polymer in [13]. This research showed an antenna that works around 3.2 GHz to 3.5 GHz and around 4 GHz to 11 GHz. Additionally, a conformal antenna was also proposed for wearable applications in [14]. This other design achieved UWB measurement from 3.6 GHz to 8.5 GHz. Moreover, simulation results of conformal UWB monopoles were presented within the frequency range from 2 GHz to 18 GHz with a band rejection from 5 GHz to 6 GHz [15] and from 3.1 GHZ to 10.6 GHz in [16].

Now, designs of antennas particularly for UAVs applications have also been proposed. For instance, antennas with a reflector were used to increase the gain at 2.4 GHz for UAV applications in [17]. A dual-polarized conformal antenna array at 9.8 GHz was proposed in [18]. A 12-element rectangular array at 2.4 GHz was installed in a fixed-wing drone [19]. The work [20] presented a planar segmented loop antenna with operation within the bands of 956 MHz, 1.8 GHz, 1.9 GHz, and 2.4 GHz. Conformal antenna array was designed with circular polarization at the frequency range

The associate editor coordinating the review of this manuscript and approving it for publication was Lu Guo.

from 1.5 GHz to 1.65 GHz [21]. A conformal circular antenna with operation at 700 MHz can be found in [22]. Besides, a conformal monopole antenna with operation at 800 MHz was studied in [23]. These antennas were specially designed for fixed-wing drones. Another example is a quadrifilar helix antenna installed on a drone tail [24]. This antenna operates with circular polarization from 865 MHz to 871 MHz and provides an isoflux pattern. It is worthy to note that above-mentioned antennas are focused on UAVs applications with a narrow frequency range, not for UWB signal detection. Recently, a conformal UWB semi-spherical antenna that works from 1.85 GHz to 10 GHz was proposed in [25]. This antenna was mounted under the center of a fixed-wing drone. It has a volumetric shape with electrical dimensions of 400mm × 200mm × 800mm. This antenna was configured for signal detection system with a conical pattern.

In this research, we now propose a linearly polarized conformal antenna to be installed on the wings of quadcopters drones for a MIMO system. The new structure is coupled to work within a UWB frequency range. This is achieved by using a Y-rounded shape with a parasitic circular element at the center of the structure. The new antenna is low-profile which is very suitable to diminish aerial vehicle drag problem when the drones are flying. The proposed antenna was simulated and measured to test its performance.

II. CONFORMAL UWB ANTENNA MODEL

The proposed design is a new conformal UWB antenna shown in Figure 1. We follow a stepwise development procedure to obtain the final design. Firstly, the initial design starts with a Y-shaped structure. Then, the structure was modified to a Y-rounded shape. In the last step of this procedure, we added a circular parasitic element located at the center of the radiating element. The Y-rounded shape element is connected to a matched feeding line which provides the current to the entire conformal antenna by means of 50 ohms SMA connector. The Y-rounded shape and the circular parasitic element provide a wider bandwidth. The final geometry is governed by equations 1, 2, and 3. These functions are used to describe the outer profile of the antenna. Besides, the antenna includes a ground plane with a small notch, as seen in Figure 1c. The antenna structure is bent in a perpendicular manner with respect to the orientation of the Y-rounded shape. This proposed structure is a low-profile antenna to facilitate its assembly on the wings of the quadcopter drone. The antenna was milled on a flexible and light circuit board called Rogers Duroid 5880LZ. The characteristics of this material are the thickness of 1.27mm, a copper layer of 35μm, permittivity of $\varepsilon_r = 1.97$ and a tangential loss of $\delta = 0.0019$.

$$f_1(x) = \begin{cases} L_b + \sqrt[+]{R_3^2 - (x - R_3 + R_1)^2} & \text{for } -R_1 \le x \le -R_2 \\ \sqrt[-]{R_2^2 - x^2} & \text{for } -R_2 < x \le R_2 \\ L_b + \sqrt[+]{R_3^2 - (x - R_1 + R_3)^2} & \text{for } R_2 < x \le R_1 \end{cases} \quad (1)$$

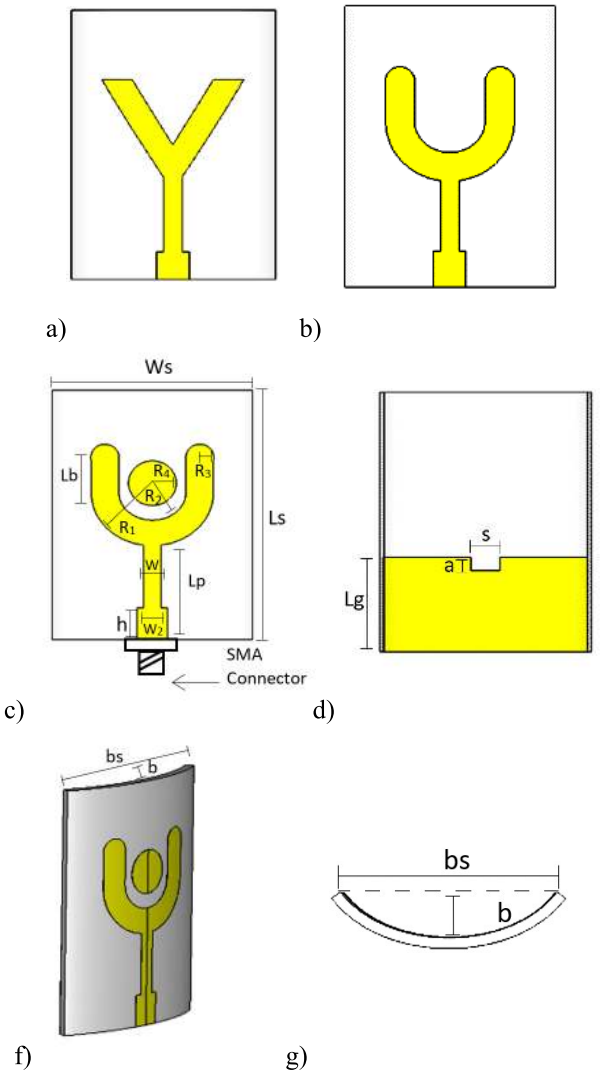

FIGURE 1. Conformal UWB Antenna: a) Y-shaped, b) Y-rounded shape, c) Y-rounded shape with parasitic element, d) ground plane, f) perspective view of conformal Y-rounded shape with parasitic element and g) top view of conformal Y-rounded shape with parasitic element.

$$f_2(x) = \sqrt[\pm]{R_4^2 - x^2} \quad \text{for } -R_4 < x \le R_4 \quad (2)$$

$$f_3(x) = \begin{cases} \sqrt[-]{R_1^2 - x^2} & \text{for } -R_1 \le x \le -w/2 \\ -L_p + h & \text{for } -w/2 < x \le w/2 \\ \sqrt[-]{R_1^2 - x^2} & \text{for } w/2 < x \le R_1 \end{cases} \quad (3)$$

A panoramic view of the proposed antenna mounted on the wing of a multirotor generic quadcopter drone is shown in Figure 2. It should be noted that the structure is perfectly assembled to the drone wing. This class of drones is convenient for UWB sensing. The main advantage of these aircraft versus modern fixed wing [25] is that they fly in a static way on a fixed place, as well as they are small, light, portable and relatively easy to manage. A UWB system mounted on these drones implies a challenge of locating the antennas on the aircraft structure [26]. The antenna cannot be located at

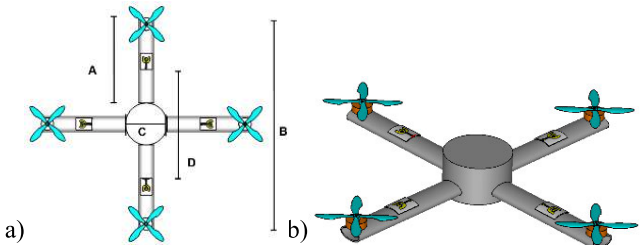

FIGURE 2. UAV model with four conformal UWB antennas: a) top view and b) perspective view.

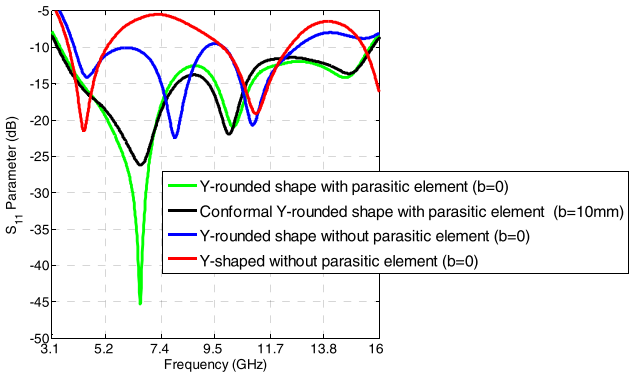

FIGURE 3. S_{11} of stepwise development procedure of the antenna.

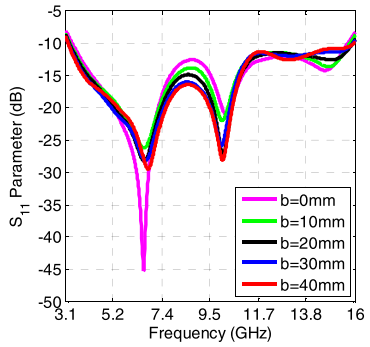

FIGURE 4. Performance of bendness b.

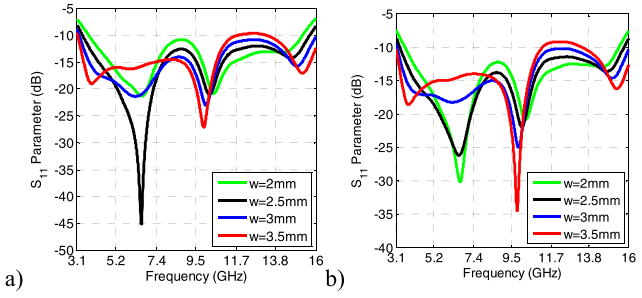

FIGURE 5. Parameter w for: a) flat antenna and b) conformal antenna.

the center of the drone, and either cannot be installed close to the wings because of the noise with the circuitry. It is preferable to locate the antenna in the middle of the wing where is the place with fewer interferences. This avoids data transmission issues in UWB communications. It was installed one antenna in each arm of the drone to add spatial diversity to

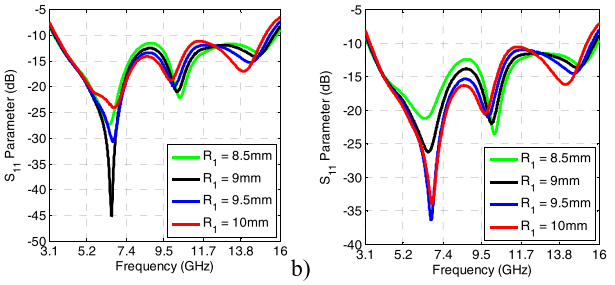

FIGURE 6. Parameter R_1 for: a) flat antenna and b) conformal antenna.

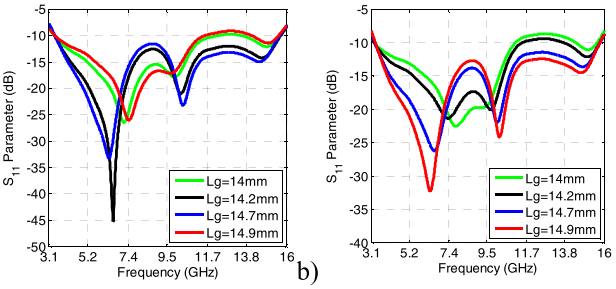

FIGURE 7. Parameter Lg for: a) flat antenna and b) conformal antenna.

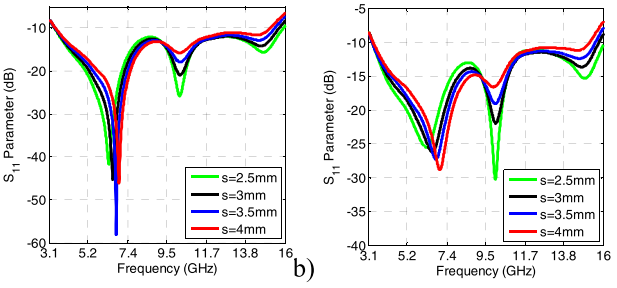

FIGURE 8. Parameter s for: a) flat antenna and b) conformal antenna.

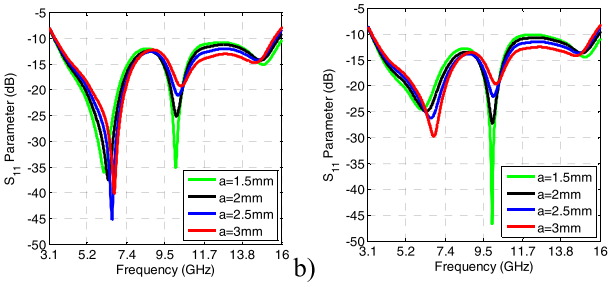

FIGURE 9. Parameter a for: a) flat antenna and b) conformal antenna.

the system [27]. The material of the drone model is fiberglass with a length of A = 20cm, B = 50cm, C = 10cm, and D = 26.1cm. This material is very common in UAV technology. The four motors were modeled by using aluminum and copper. The value of spacing D was strategically selected to minimize mutual coupling between the antennas.

III. SIMULATION AND EXPERIMENTAL RESULTS

The physical parameters of the new structure were configured by running several simulations with the CST Microwave

TABLE 1. Dimensions of the UWB antenna in mm.

Ws	Lb	R_4	R_2	R_3	R_1	w	w_2
29	4.5	2.8	3.5	3.25	10	3	4.5
h	**Lp**	**Lg**	**a**	**s**	**b**	**bs**	**Ls**
5	10	14.7	2	3	10	28.1	39

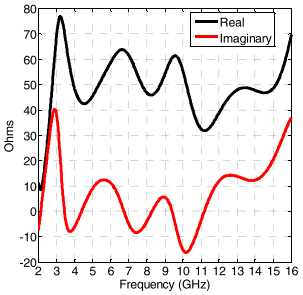

FIGURE 10. Input impedance.

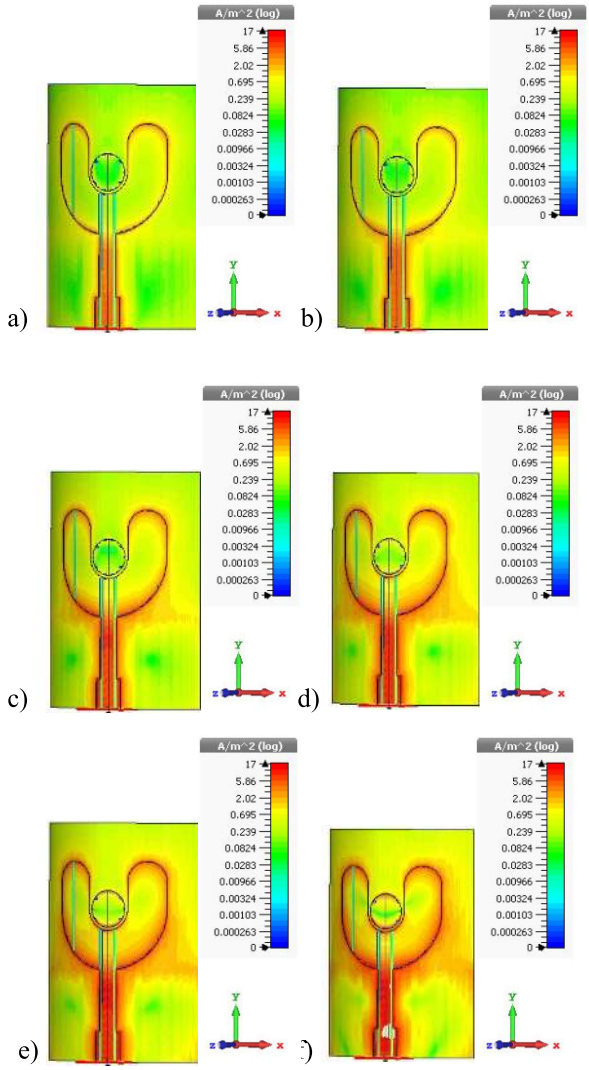

FIGURE 11. Front side current distribution: a) 3.43 GHz, b) 4.38 GHz, c) 6.72 GHz, d) 8.29 GHz, e) 9.39 GHz and f) 11.18 GHz.

Studio Software. Figure 3 shows the S_{11} parameter of the antennas depicted in Figure 1. The designs with no parasitic element do not work within the whole UWB range.

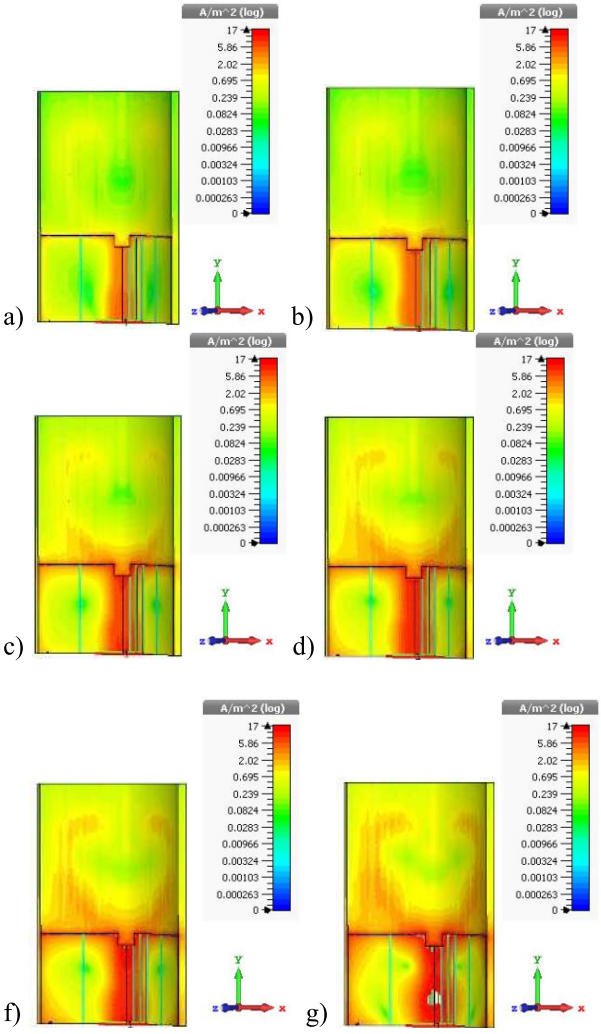

FIGURE 12. Back side current distribution: a) 3.43 GHz, b) 4.38 GHz, c) 6.72 GHz, d) 8.29 GHz, e) 9.39 GHz and f) 11.18 GHz.

Nonetheless, the parasitic circular element helps to increase the bandwidth even if the structure is bent.

After the above procedure, the final structure was slightly bent by varying the parameter b. Figure 4 shows the S_{11} parameter under -10dB for different values of b. The proposed antenna keeps the UWB performance when the structure is bent.

The width of the first microstrip feed line w is part of the distribution of the current to the radiator patch. It is an important parameter for the design of the conformal UWB antenna; it mainly distributes current along with the patch. As shown in Figure 5, the structure was simulated for different parametric values of w. We observed that the reflection coefficient varies considerably. When this parameter is 3 mm, the antenna is tuned over the entire established frequency range. The parameters R_1 and R_2 define the spacing between the parasitic element and the U-shaped. The circular parasitic element is coupled with the U-shaped element and has a radius defined by the variable R_4. These parameters were also modified by using different values where it is found

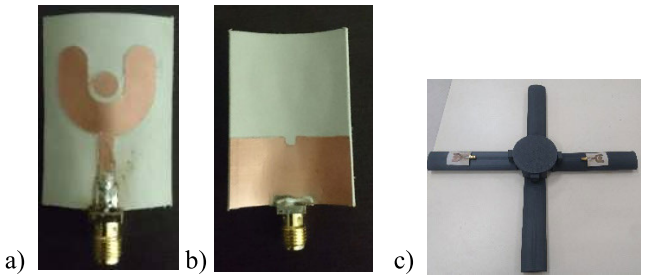

FIGURE 13. Prototype: a) front view, b) back side and c) antenna on UAV model.

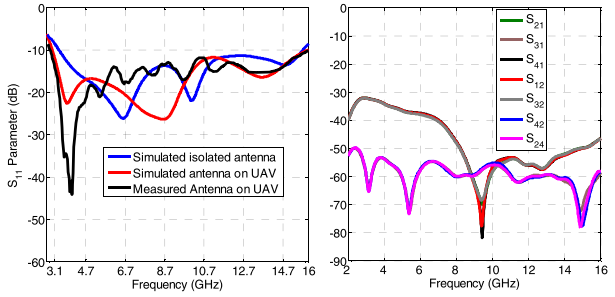

FIGURE 14. S-parameters of the UWB antenna: a) reflection coefficient and b) coupling coefficients.

that the S_{11} parameter does not have a significant change in lower frequencies. The reflection coefficient only changes slightly in higher frequencies as depicted in Figure 6. The ground plane of the antenna is a rectangular metallization with an upper notch that provides certain miniaturization of the antenna. The size of the parameter Lg affects the performance of the antenna considerably, as depicted in Figure 7. It is preferable to tune the antenna with a slightly wider ground plane. Figures 8 and 9 show the performance of antenna when the notch is tuned, the parameters a and s does not affect substantially in the low frequencies. These parameters only affect high frequencies. As a result of this parametric study, we selected the final parameters presented in Table 1. It is worthy to note that the remaining parameters were constant during this parametric study.

Figure 10 shows the input impedance of the antenna. The propagating modes are found when the imaginary part of the impedance is zero. Hence, the modes correspond to the following resonance frequencies: 3.43 GHz, 4.38 GHz, 6.72 GHz, 8.29 GHz, 9.39 GHz and, 11.18 GHz. The average current distributions for the propagating modes are shown in Figures 11 and 12 for both sides. In this case, the current flows on the metallization with different levels for each frequency. The level of current increases in high frequencies. As expected, the current is concentrated in the periphery of the profile. The curvature of the antenna helps to increase the bandwidth. The antennas are mounted on the UAV, do not generate any current flow on the aircraft.

The antenna was fabricated according to the dimensions of Table 1. The corresponding prototype is depicted in

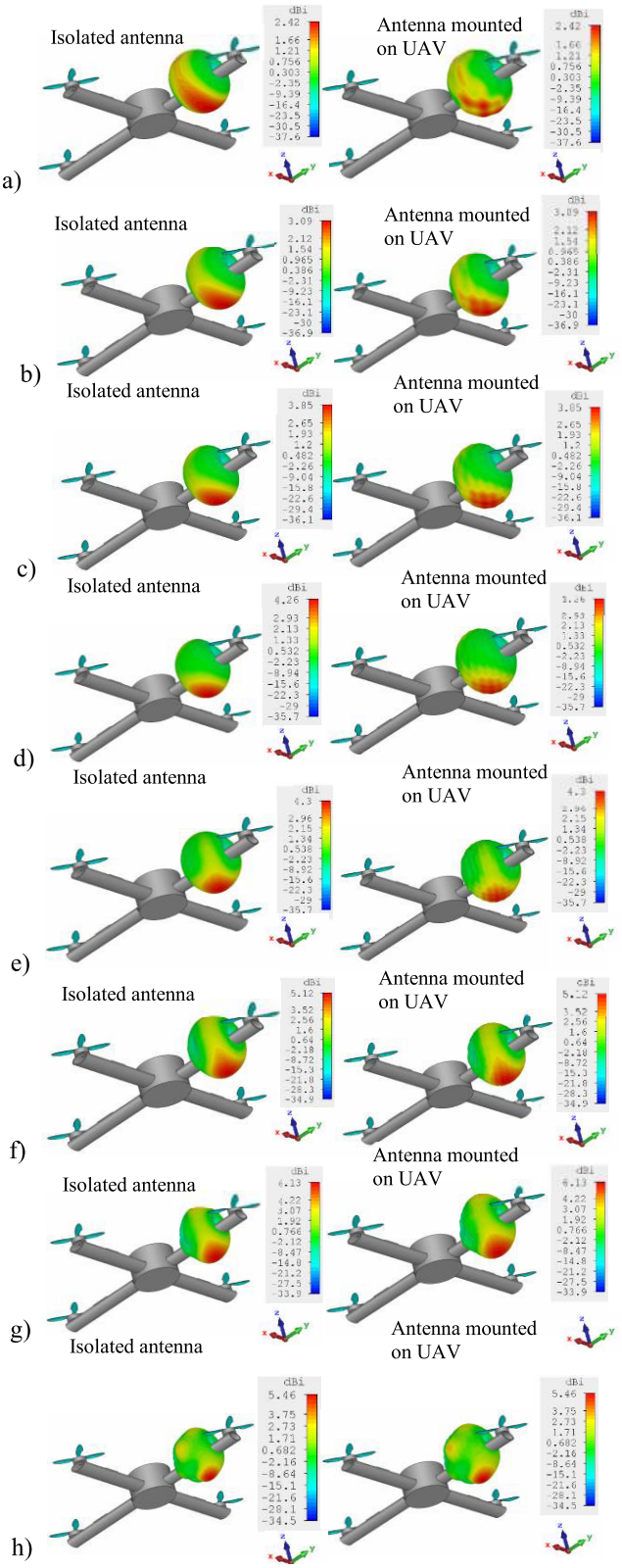

FIGURE 15. 3D patterns on UAV at: a) 3.1 GHz, b) 4.1GH z, c) 5.1 GHz d) 6.1 GHz, e) 7.1 GHz, f) 8.1 GHz, g) 9.1 GHz and h) 10.1 GHz.

Figure 13a and 13b. After the fabrication process, we measured the UWB antenna mounted on the aircraft structure, as shown in Figure 13c. As a result of this, Figure 14a

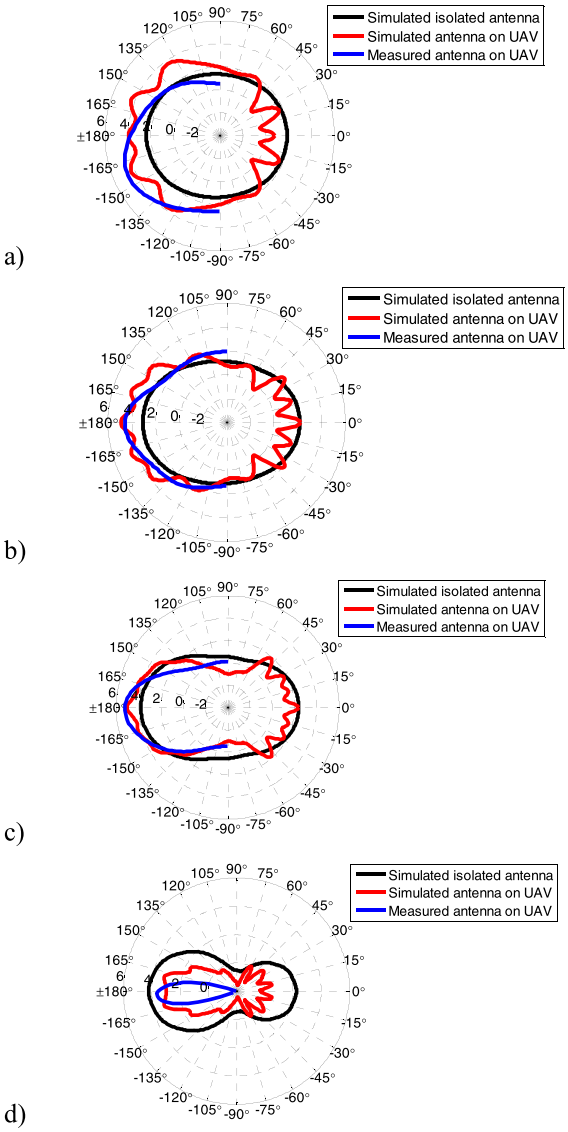

FIGURE 16. 2D patterns versus θ angle in dBi of YZ-plane at: a) 3.1 GHz, b) 4.1 GHz, c) 5.1 GHz and d) 6 GHz.

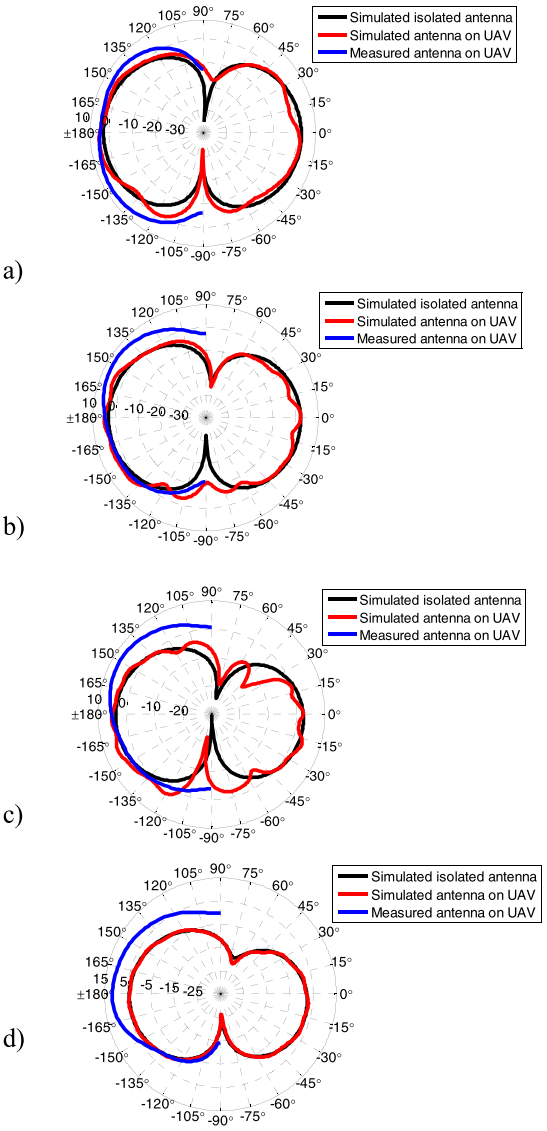

FIGURE 17. 2D patterns versus θ angle in dBi of XZ-plane at: a) 3.1 GHz, b) 4.1 GHz, c) 5.1 GHz and d) 6 GHz.

shows the comparison of the measurement and simulated S_{11} parameter when the antenna is isolated as well as when the antenna is on the UAV structure. It was found that the measured antenna works perfectly from 2.9 GHz to 15.9 GHz. The measured reflection coefficient was obtained by using a calibrated network analyzer R&S model ZNB20.

For any UWB MIMO system, it is essential the isolation of the antennas. In this case, Figure 14b depicts the coupling coefficients of four antennas mounted on the UAV. The levels of these parameters are under −30dB in all UWB range. The radiation patterns are illustrated in Figures 15, 16 and 17. As it can be observed the antenna provides the maximum radiation towards down of the aircraft structure, this is very suitable for exploration above the earth with UAVs. This type of radiation can communicate to any user on the earth. The antennas are strategically located in order to save space in the center of the drone and to add the spatial diversity to the system. It is worthy to note that this is one of the technical challenges in quadcopter drones. Placing the antennas on this location, it is possible to mount four antennas in the aircraft structure for a UWB system. Figure 16 illustrates the 3D views of simulated radiation patterns when the UAV structure is excluded and included during the simulation. Note that the radiation patterns are slightly distorted for low frequencies when the UAV structure is included in the simulation. However, the pattern distortion is more noticeable in high frequencies. Moreover, the maximum radiation remains towards the ground directly in the patterns from 3.1 GHz to 10.1 GHz. Nonetheless, there is a change of 90 degrees of the maximum radiation in the patterns from 11.1 GHZ to 15.1 GHz. The fiberglass of the drone model affects the performance of the radiation pattern until 10.1 GHz. As conjecture of this performance,

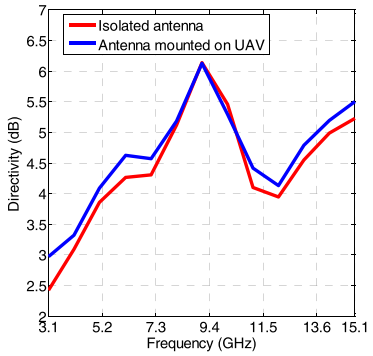

FIGURE 18. Directivity of the antenna.

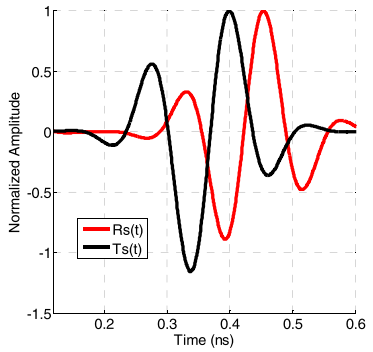

FIGURE 19. Time signals at $\theta = 180°$.

TABLE 2. System fidelity factor.

θ	SFF
160º	0.9785
170º	0.9820
180º	0.9833
190º	0.9820
200º	0.9785

the antennas can detect signals coming from the ground directly in low frequencies and coming from the surrounding of the UAV in the azimuth plane for high frequencies. Hence, the acceptable radiation pattern performance is until 10.1 GHz for exploration flights because the UWB system mounted on the UAV would be detecting signals coming from the earth.

In this case, Figures 16 and 17 show the 2D patterns in terms of elevation angle θ for the main radiation cuts, i.e., the YZ-plane ($\varphi = 90°$) and XZ-plane ($\varphi = 0°$) from 3.1 to 6 GHz. There are acceptable differences in the patterns. However, it demonstrates the excellent operation of the antenna. It was used the EMSCAN equipment to measure the radiation patterns. This equipment can only measure the half radiation pattern of the antenna until 6 GHz [29].

Now, Figure 18 depicts the maximum directivity of the antenna in the 3D patterns versus frequency. The red line corresponds to the antenna in isolation, i.e., without the drone model. The blue line is the directivity of the antenna when it

TABLE 3. Comparison of antennas.

Type	Application	Size	Material	Frequency / Polarization
Flat ([3])	Wifi on Fixed wing UAV	15.5 cm ×2.08 cm	FR4	2.4 GHz / Linear
Flat ([4])	Fixed wing UAV	71 cm×25 cm	Sheet of copper	20-1200 MHz / Linear
Flat ([5])	Fixed wing UAV	Radius = 47.2 mm.	Arlon AD250 A	2.67 GHz / Linear
Flat Array ([6])	Wifi on Fixed wing UAV	Patch = 36×28 mm Array = 396mm^2	FR4	2.45 GHz / Linear
Flat ([7])	Indoor positioning system on quadcopter UAV	44mm × 29 mm	DecaWave ScenSor DWM1000 module	6.48 GHz / Linear
Flat ([17])	Fixed wing UAV	Radius 80mm	FR-4	2.45 GHz / Linear
Conformal array ([18])	UAV fixed wing with Polarimetric radars	20.8cm × 22.7cm	Rogers 5880	9.8 GHz / Linear dual
Flat array ([19])	Wifi on Fixed wing UAV	458.8 mm × 161mm	RO4350	2.4 GHz / Linear
Flat segmented loop ([20])	GPS, GSM, UMTS, LTE and ISM communications on a fixed wing UAV	75 mm × 75 mm	FR4	956 MHz and from 1.5 GHz to 2.6 GHz / Linear
Conformal array ([21])	Fixed wing UAV	240 mm ×150 mm	Metal	1.5 GHz to 1.65 GHz / circular
Conformal ([22])	Fixed wing UAV	45mm	PEC	700 MHz / /Linear
Conformal ([23])	Fixed wing UAV	130.8 × 20mm × 90mm	Sheet of copper	807 – 835 MHz / Linear
Quadrifilar Helix ([24])	Fixed wing UAV telemetry and remote-control systems.	0.127 mm× 238.4 mm× 69.1 mm	Nelco NY9217	0.85–0.89 GHz / Circular

TABLE 3. ***(Continued.)*** **Comparison of antennas.**

Conformal ([25])	UWB Signal detection on fixed wing UAV.	400 mm × 200 mm	Sheet of copper	1.85 to 10 GHz / Linear
Proposed antenna	UWB MIMO system on quadcopter UAV.	29mm × 39mm	Rogers 5880LZ	2.9 GHz to 10.1 GHz / Linear

is mounted on the UAV model. The presence of the UAV body does not affect substantially the directivity of the antenna. In fact, it is slightly increased when the antenna is mounted on the drone structure. Otherwise, following the mathematical procedure of [28], we computed the system transfer function in MATLAB by extracting the S_{11} parameter, radiated E-field phase and, gain versus frequency from CST software. Then, it was computed the system fidelity factor (SFF) by modeling the cross-correlation between the normalized receiving (Rs(t)) and transmitting (Ts(t)) pulses. These pulses are illustrated in Figure 19. Table 2 contains the SFF for five directions of θ in the plane YZ ($\varphi = 90°$). The antenna has an SFF>0.9 for $\theta = 160°$, $\theta = 170°$, $\theta = 180°$, $\theta = 190°$, and $\theta = 200°$. These are the directions of the significant concentration of power, as observed in Figures 15 and 16. Finally, Table 3 presents a comparison of UAV antennas of state of the art and the proposed design in this research. This antenna solution is the right candidate for a UWB system mounted drones. The main differences of this design in comparison with the literature are the frequency range, spatial diversity for UWB MIMO systems, the low profile, type of radiation that it is concentrated towards the ground direction and the application for small quadcopters drones.

IV. CONCLUSION

This paper presented a new linearly polarized antenna design for UWB communications. The main advantages of the proposed antenna are the aerodynamic shape for quadcopter drones, low-profile, and UWB operation. With this geometry, the drag problem can be diminished during the flights. This new antenna is a good alternative for UWB systems with drones because there exists the possibility to use four antennas on the aircraft. This can avoid generating interferences with the circuitry of the whole system. The fabricated prototype was mounted in a real aircraft structure and provided a similar performance of the simulated antenna. Future works will be focused on the implementation of a UWB system during the flight of a UAV.

REFERENCES

[1] J. Li and P. Stoica, "MIMO radar with colocated antennas," *IEEE Signal Process. Mag.*, vol. 24, no. 5, pp. 106–114, Sep. 2007.

[2] M. García-Fernández, Y. Á. LÃ pez, A. Arboleya, B. González-Valdés, Y. Rodríguez-Vaqueiro, M. E. De C. Gómez, and F. L.-H. AndrÃĪs, "Antenna diagnostics and characterization using unmanned aerial vehicles," *IEEE Access*, vol. 5, pp. 23563–23575, 2017.

[3] M. S. Sharawi, D. N. Aloi, and O. A. Rawashdeh, "Design and implementation of embedded printed antenna arrays in small UAV wing structures," *IEEE Trans. Antennas Propag.*, vol. 58, no. 8, pp. 2531–2538, Aug. 2010.

[4] M. Nosrati, A. Jafargholi, and N. Tavassolian, "A broadband blade dipole antenna for UAV applications," in *Proc. IEEE Int. Symp. Antennas Propag. (APSURSI)*, Fajardo, Puerto Rico, Jun./Jul. 2016, pp. 1777–1778.

[5] L. Sun, B.-H. Sun, Q. Sun, and W. Huang, "Miniaturized annular ring slot antenna for small/mini UAV applications," *Prog. Electromagn. Res.*, vol. 54, pp. 1–7, Oct. 2014.

[6] M. S. Sharawi, M. Ibrahim, S. Deif, and D. N. Aloi, "A planar printed antenna array embedded in the wing structure of a UAV for communication link enhancement," *Prog. Electromagn. Res.*, vol. 138, pp. 697–715, Apr. 2013.

[7] J. Tiemann, F. Schweikowski, and C. Wietfeld, "Design of an UWB indoor-positioning system for UAV navigation in GNSS-denied environments," in *Proc. Int. Conf. Indoor Positioning Indoor Navigat. (IPIN)*, Banff, AB, Canada, Oct. 2015, pp. 1–7.

[8] Z. Yin, Z. Shi, J. Liang, and Z. Wu, "Design of unmanned aerial vehicle space communication links based on DS-UWB," *Inf. Technol. J.*, vol. 9, no. 8, pp. 1713–1718, 2010.

[9] F. B. Sorbelli and C. M. Pinotti, "On the localization of sensors using a drone with UWB antennas," in *Proc. RSFF*, L'Aquila, Italy, Jul. 2018, pp. 18–29.

[10] J. Chen, D. Raye, W. Khawaja, P. Sinha, and I. Guvenc, "Impact of 3D UWB antenna radiation pattern on air-to-ground drone connectivity," in *Proc. IEEE 88th Veh. Technol. Conf.*, Aug. 2018, pp. 1–5.

[11] D. Gaetano, M. J. Ammann, P. McEvoy, M. John, L. Keating, and F. Horgan, "Proximity study of a conformal UWB directional antenna on water pipe," *Microw. Opt. Technol. Lett.*, vol. 54, no. 8, pp. 1982–1986, 2012.

[12] S. Mondal and P. P. Sarkar, "Design of an ultrawideband conformal metal antenna," *Microw. Opt. Technol. Lett.*, vol. 56, no. 2, pp. 430–434, 2014.

[13] S. Nikolaou, G. E. Ponchak, J. Papapolymerou, and M. M. Tentzeris, "Conformal double exponentially tapered slot antenna (DETSA) on LCP for UWB applications," *IEEE Trans. Antennas Propag.*, vol. 54, no. 6, pp. 1663–1669, Jun. 2006.

[14] M. H. Sagor, Q. H. Abbasi, A. Alomainy, and Y. Hao, "Compact and conformal ultra wideband antenna for wearable applications," in *Proc. 5th Eur. Conf. Antennas Propag. (EUCAP)*, Rome, Italy, Apr. 2011, pp. 2095–2098.

[15] E. S. Ahmed, "Conformal band-notch UWB monopole antenna on finite cylindrical substrates," *ETASR Eng. Technol. Appl. Sci. Res.*, vol. 3, no. 3, pp. 440–445, 2013.

[16] M. Ahmed, D. K. Das, and A. Rahman, "Study of a conformal UWB antenna designed on various non-planar surfaces," in *Proc. Loughborough Antennas Propag. Conf. (LAPC)*, Loughborough, U.K., Nov. 2012, pp. 1–5.

[17] M. S. B. Safaron, H. A. Majid, B. A. F. Esmail, A. S. Ab Ghafar, F. A. Saparudin, M. F. Ismail, and M. A. B. Abdullah, "Directional cloverleaf antenna for unmanned aerial vehicle (UAV) application," *Indonesian J. Electr. Eng. Comput. Sci.*, vol. 14, pp. 773–779, May 2019.

[18] C.-H. Ahn, Y.-J. Ren, and K. Chang, "A dual-polarized cylindrical conformal array antenna suitable for unmanned aerial vehicles," *Int. J. RF Microw. Comput.-Aided Eng.*, vol. 21, no. 1, pp. 91–98, 2011.

[19] S. Dweik, S. Deif, W. Sadeh, O. A. Rawashdeh, D. N. Aloi, and M. S. Sharawi, "A planar antenna array with integrated feed network for UAV applications," in *Proc. Eur. Conf. Antennas Propag.*, Apr. 2014, pp. 1855–1858.

[20] D. Kang, J. Tak, and J. Choi, "Wideband low-profile planar square segmented loop antenna for UAV applications," *Electron. Lett.*, vol. 52, no. 22, pp. 1828–1830, Oct. 2016.

[21] Z. Wei and Y. Junfeng, "A design of vertical polarized conformal antenna and its array based on UAV structure," *Int. J. Antennas Propag.*, vol. 2017, pp. 1–12, Oct. 2017.

[22] S. Yoon, J. Tak, J. Choi, and Y.-M. Park, "Conformal monopolar antenna for UAV applications," in *Proc. IEEE Int. Symp. Antennas Propag., USNC/URSI Nat. Radio Sci. Meeting*, San Diego, CA, USA, Jul. 2017, pp. 517–518.

[23] Z.-Q. Liu, Y.-S. Zhang, Z. Qian, Z. P. Han, and W. Ni, "A novel broad beamwidth conformal antenna on unmanned aerial vehicle," *IEEE Antennas Wireless Propag. Lett.*, vol. 11, pp. 196–199, 2012.

[24] J.-M. F. Gonzalez, P. Padilla, J. F. Valenzuela-Valdes, J.-L. Padilla, and M. Sierra-Perez, "An embedded lightweight folded printed quadrifilar helix antenna: UAV telemetry and remote control systems," *IEEE Antennas Propag. Mag.*, vol. 59, no. 3, pp. 69–76, Jun. 2017.

[25] J.-Y. Jeong and J.-M. Woo, "Ultra-wide band antenna attachable on UAV surface," *Int. J. RF Microw. Comput.-Aided Eng.*, vol. 27, no. 8, pp. 1–7, 2017.
[26] R. L. Musselman, "Antenna design for small UAV locator applications," in *Proc. Amer. Soc. Eng. Educ.*, Jun. 2017, pp. 1–10.
[27] T. Kaiser, F. Zheng, and E. Dimitrov, "An overview of ultra-wide-band systems with MIMO," *Proc. IEEE*, vol. 97, no. 2, pp. 285–312, Feb. 2009.
[28] G. Quintero, J. F. Zurcher, and A. K. Skrivervik, "System fidelity factor: A new method for comparing UWB antennas," *IEEE Trans. Antennas Propag.*, vol. 59, no. 4, pp. 2502–2512, Jul. 2011.
[29] *EMSCAN*. Accessed: Sep. 9, 2019. [Online]. Available: http://emscan.com/products/antenna-testing/

LUZ I. BALDERAS received the degree in computational systems engineering and the M.S. degree in electrical and electronic engineering from the University Autonomous of Tamaulipas, in 2006 and 2009, respectively, where she is currently pursuing the Ph.D. degree in electrical and electronic engineering. Her main research interest includes the design and optimization of ultrawideband antennas.

ALBERTO REYNA was born in San Fernando, Mexico, in 1982. He received the M.S. degree in electronics communications from the University of Tamaulipas, Reynosa, Mexico, and the Ph.D. degree in communications technologies from the Public University of Navarre, Pamplona, Spain. He is currently with the University Autonomous of Tamaulipas, Mexico and Radanter SA DE CV. His current interests include antenna arrays, ultrawideband antennas, optimization, and energy harvesting.

MARCO A. PANDURO received the M.S. degree in electronics of high frequency and the Ph.D. degree in electronics and telecommunications from the CICESE Research Center, Ensenada, Mexico, in 2001 and 2004, respectively. He was a Professor with the Communications Department, University Autonomous of Tamaulipas (UAT), from 2005 to 2015. He is currently with the CICESE Research Center. His current interests include antenna arrays, smart adaptive antennas, microwave devices, and optimization via different evolutionary algorithms.

CARLOS DEL RIO was born in Reus, Spain, in 1970. He received the Ingeniero Tècnico de Telecomunicación degree from Ramon Lull University, Barcelona, in 1991, the Electronic Engineer degree, in 1998, and the Ph.D. degree (Hons.) in telecomunicación from the Public University of Navarra, in 1996. Since 1993, he has been developing his research and docent activities at the Electric and Electronic Engineering Department, Public University of Navarra, where he is currently an Associate Professor. His research interests include horn antenna design in general, satellite and terrestrial communications, study of periodic metallo-dielectric structures, also known as electromagnetic bandgaps structures, development of numerical computation software based on mode matching and scattering matrix, antenna measurements, far- and near-field measurement chambers, compact ranges, and so on.

ARNULFO R. GUTIÉRREZ received the degree in electrical engineering from the Instituto Tecnológico de Ciudad Madero, in 1998, and the master's degree in industrial and business administration from the Universidad Autónoma de Nuevo León, in 2008. He is currently pursuing the Ph.D. degree in electrical and electronic engineering with the University Autonomous of Tamaulipas. His main research interests include the design of SIW antenna arrays and evolutionary optimization.